

# THE COMMON SELF-POLAR TRIANGLE OF SEPARATE CIRCLES: PROPERTIES AND APPLICATIONS TO CAMERA CALIBRATION

*Haifei Huang*<sup>1,2</sup>     *Hui Zhang*<sup>2</sup>     *Yiu-ming Cheung*<sup>1,2</sup>

<sup>1</sup>Department of Computer Science, Hong Kong Baptist University, Hong Kong SAR, China

<sup>2</sup> United International College, BNU-HKBU, Zhuhai, China

## ABSTRACT

This paper investigates the properties of the common self-polar triangle of separate coplanar circles and applies them to camera calibration. We find that any two separate circles have a unique common self-polar triangle. In particular, we show that one vertex of the common self-polar triangle lies on the line at infinity. Given three separate circles, the line at infinity can be recovered using the vertices of the common self-polar triangles. Accordingly, the vanishing line of the support plane can be obtained in their images. This allows recovering the imaged circular points, which provides good constraints on the image of the absolute conic. Compared to previous calibration methods using separate circles, our approach can avoid solving quartic equation, which often causes numerical instability. In the application, we test one calibration algorithm and accurate results are achieved.

*Index Terms*— Calibration, Circle, Self-polar triangle

## 1. INTRODUCTION

Camera calibration is an active topic in computer vision [1, 2, 3, 4, 5, 6, 7, 8], which is an essential step for inferring metric information from 2D images. Traditional calibration methods always require highly accurate tailor-made 3D objects and an elaborate setup. As the camera is becoming cheap and popular, an easy and flexible calibration technique is needed for non-experts to perform simple vision tasks. To this end, there are two popular types of 2D patterns used in camera calibration. The first one is grid pattern. For instance, Zhang [4] used a planar grid pattern in camera calibration and achieved accurate results. However, point matching is required and needs to be done manually. To avoid this, the second type is circular pattern. In [9], Meng et al. have proposed a method using a pattern that consists of a circle and straight lines passing through its centers. In [10], Chen et al. have provided a novel camera calibration method to estimate the extrinsic parameters and the focal length of a camera using only one single

image of two coplanar circles with arbitrary radius.

In this paper, we focus on the separate coplanar circles pattern (see Fig.1). To avoid ambiguity, separate in this paper means disjoint and not enclosing. In [11], Wu et al. discussed different coplanar circles pattern and conducted experiments using separate circles. According to their method, they solved quartic equation, and selected imaged circular points (ICPs) using quasi-affine invariance. However, Kim et al. [12] pointed out that, without any other consideration, finding complex roots of quartic equation may cause numerical instability. Unfortunately, there is no discussion on this issue in their paper. Consequently, it is hard to repeat their experiments. In paper [13], Gurdjos et al. presented an approach for recovering the Euclidean structure (Imaged Circular Points) from two or more parallel circles. In order to obtain linear solutions, they considered degenerate conics spanned by two circles. They demonstrated that each degenerate conic can be decomposed into two distinct lines. Then, they use the absolute signature to identify two special lines in one degenerate conic, each of which is determined by a pair of complex conjugate points. After obtaining two special lines, they used the limit points to determine which line is the line at infinity. Once the three degenerate conics can be distinguished, then constraints on absolute degenerate conic are used to achieve a linear solution for the imaged circular points. However, this method involved complex theory and is not geometrically intuitive and direct. In this paper, we tackle this problem using the common self-polar triangle of separate coplanar circles. We find that any two separate circles have a unique common self-polar triangle. In particular, one vertex of the common self-polar triangle lies on the line at infinity. Given three separate circles, the line at infinity can be recovered using the vertices of the common self-polar triangles. Accordingly, the vanishing line of the support plane can be obtained in their images. This allows to recover the imaged circular points, which provides good constraints on the image of absolute conic. The calibration method has three advantages: (1) Pole-polar relationship is a simple and common theory in projective geometry. (2) There is no point matching. (3) There is no quartic equation solving. In the application, we test one calibration algorithm and accurate results are achieved.

In our previous work, we have explored the properties of

This work was partially supported by the National Natural Science Foundation of China (Project no. 61005038 and 61272366) and internal funding from BNU-HKBU United International College (Project no. R201312 and R201616). Thanks to Mr. Chen Quanxin for the reconstruction of the vase.



**Fig. 1.** Separate Coplanar Circles.

the common self-polar triangle of concentric circles [14] and sphere images [15]. The difference between this paper and [15] is that, in [15], the circles obtained from the occluding contours of spheres are not coplanar, and the line passing through the camera and each circle center is orthogonal to the support plane. In this paper, all circles are coplanar, and no such orthogonality exists. To the best of our knowledge, in existing literature, there is no research on the properties of the common self-polar triangle of the separate coplanar circle images.

The remainder of this paper is organized as follows. Section 2 briefly introduces some notations and theorems. Section 3 discusses the properties of common self-polar triangle of separate circles. Section 4 describes calibration methods. Section 5 shows the experimental results on synthetic and real data sets. Finally, a conclusion is drawn in Section 6.

## 2. PRELIMINARIES

### 2.1. Camera Model and Circular Points

In this paper, we adopt pinhole camera model. The intrinsic parameters of pinhole camera can be represented by

$$\mathbf{K} = \begin{bmatrix} \alpha f & s & u_0 \\ 0 & f & v_0 \\ 0 & 0 & 1 \end{bmatrix}. \quad (1)$$

In the matrix  $\mathbf{K}$ ,  $f$  is the focal length,  $\alpha$  is the aspect ratio,  $(u_0, v_0)$  is the principal point, and  $s$  is the skew. Let  $\mathbf{M} = [X \ Y \ Z \ 1]^T$  be a world point and  $\mathbf{m} = [x \ y \ 1]^T$  be its image. The imaging process can be represented as

$$u\mathbf{m} = \mathbf{K}[\mathbf{R}|\mathbf{t}]\mathbf{M}, \quad (2)$$

where  $u$  is a nonzero scale factor, and  $\mathbf{R}|\mathbf{t}$  denotes a rigid transformation.

In projective geometry, any circle in a plane intersects the line at infinity of the plane at two points, which are called circular points. The image of the circular points lie on the image of the absolute conic  $\omega$  (IAC), which can be represented by  $\mathbf{K}^{-T}\mathbf{K}^{-1}$  [16]. Once the  $\omega$  is determined, the intrinsic parameters  $\mathbf{K}$  can be determined by Cholesky decomposition [17].

### 2.2. Pole-polar Relationship and Self-polar Triangle

A point  $\mathbf{x}$  and conic  $\mathbf{C}$  define a line  $l = \mathbf{C}\mathbf{x}$ . The line  $l$  is called the polar of  $\mathbf{x}$  with respect to  $\mathbf{C}$ , and the point  $\mathbf{x}$  is the pole of  $l$  with respect to  $\mathbf{C}$ .

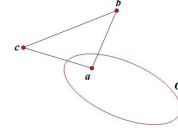


**Fig. 2.**  $\triangle abc$  is a self-polar triangle with respect to conic  $\mathbf{C}$  when polars of  $a$ ,  $b$  and  $c$  are lines  $bc$ ,  $ac$  and  $ab$ , respectively.

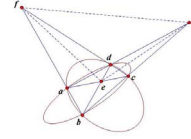


**Fig. 3.** The diagonal triangle  $efg$  of the quadrangle  $abcd$  is a common self-polar triangle for the two conics.

If the poles of a conic form the vertices of a triangle and their respective polars form its opposite sides, it is called a self-polar triangle (see Fig.2). If a self-polar triangle is common to two conics, it is called common self-polar triangle (see Fig.3) [18].

For the sake of discussion in the coming sections, we recalled three theorems related to pole-polar here. Proof and more details could be found in [16] [19] [20]. They are:

**Theorem 1.** If  $\mathbf{x}$  is on the polar of  $\mathbf{y}$  then  $\mathbf{y}$  is on the polar of  $\mathbf{x}$ .

**Theorem 2.** If  $a, b, c, d$  are four points on the conic, the diagonal triangle  $efg$  of the quadrangle  $abcd$  is self-polar triangle for the conic (see Fig.3).

**Theorem 3.** If two conics intersect in four distinct points, they have one and only one common self-polar triangle (see Fig.3).

## 3. THE COMMON SELF-POLAR TRIANGLE OF SEPARATE CIRCLES

Before exploring the properties of the common self-polar triangle of separate circles, one proposition is established below.

**Proposition 1.** Two separate circles have a unique common self-polar triangle.

**Proof.** Considering intersection points of two separate circles, it is easy to find that they have four imaginary intersection points, which fall into two conjugate pairs. Obviously, these four intersection points are distinct. According to the Theorem 3 in Section 2, we can conclude that two separate circles have a unique common self-polar triangle.

### 3.1. Properties of the Common Self-polar Triangle

Based on the fact that two separate circles have a unique common self-polar triangle, we investigate the properties and following results are achieved.

**Property.** One vertex of the common self-polar triangle of

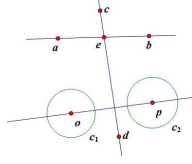


**Fig. 4.** One vertex of the common self-polar triangle for circles  $C_1$  and  $C_2$  is point  $e$ , which is the intersection point of the line at infinity  $ab$  and line  $cd$ . Obviously, point  $e$  is on line  $ab$ .

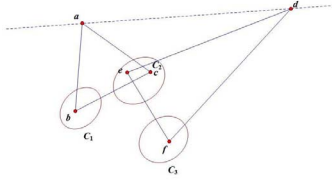


**Fig. 5.** Vanishing line  $ad$  of the support plane recovered from vertices of common self-polar triangle of circle images.

two separate circles lies on the line at infinity. The opposite side of the vertex goes through the centers of the two circles.

**Proof.** Let  $o, p$  be the centers of two circles  $C_1, C_2$ , and points  $a, b, c, d$  are imaginary intersection conjugate points of  $C_1, C_2$  (see Fig.4). Due to the fact that any two circles intersect the line at infinity at two circular points, we can assume that points  $a$  and  $b$  are the circular points. Then, the line  $ab$  is the line at infinity. According to Theorem 2 in Section 2, the common self-polar triangle is the diagonal triangle of the quadrangle  $abcd$ , we can conclude that one vertex of the common self-polar triangle is the intersection point  $e$  of lines  $ab$  and  $cd$ . Obviously, this vertex lies on the infinite line  $ab$ . Further more, the infinite line is the polar of both  $o$  and  $p$ . In terms of Theorem 1 in Section 2, we obtain that the polar of  $e$  goes through the centers of the two circles.

### 3.2. Recovery of the Vanishing Line

As we know, pole-polar relationship is an invariant under projective transformation and the image of the infinite line is the vanishing line. Based on the analysis in Subsection 3.1, we have that the images of two separate circles have a unique common self-polar triangle, and one vertex of the common self-polar triangle lies on the vanishing line. Considering an image of three separate circles, any two of them have a unique common self-polar triangle and each common self-polar triangle has a vertex on the vanishing line. Then, the vanishing line can be recovered from vertices of at least two common self-polar triangles (see Fig.5).

### 3.3. Recovery of the Vertices

There is still a problem in Subsection 3.2, which is how to recover the vertices of the common self-polar triangle. Let the images of two separate circles be  $C_1$  and  $C_2$ , and if there exists a common pole  $x$  and polar  $l$ , the following relationship should be satisfied:

$$\begin{aligned} l &= C_1 x \\ l &= \lambda C_2 x, \end{aligned} \quad (3)$$

where  $\lambda$  is a scalar parameter. Subtracting the equations in (4), we get  $(C_1 - \lambda C_2)x = 0$ . By multiplying the inverse of  $C_2$  on both sides, we obtain the following equation:

$$(C_2^{-1}C_1 - \lambda I)x = 0. \quad (4)$$

From the equation of (4), we find the common poles for  $C_1$  and  $C_2$  are the eigenvectors of  $C_2^{-1}C_1$ .

## 4. APPLICATION: A LINEAR APPROACH TO CAMERA CALIBRATION

Based on the above analysis, this section introduces a linear approach to solve the problem of calibration.

### 4.1. Recovery of Imaged Circular Points

In Section 2, we have mentioned the image of the circular points play an important role in camera intrinsic parameters estimation. Based on the properties described in Section 3, we briefly summarize the procedure for recovering imaged circular points below:

- Step 1.** Obtain circle images  $C_1, C_2$  and  $C_3$ .
- Step 2.** Calculate vertices of the common self-polar triangle for the three pairs of circle images  $C_1, C_2$  and  $C_3$  using (4).
- Step 3.** Find vertices outside of the circle images and connect any two of them.
- Step 4.** Detect the ICs by calculating the intersection points of the circle image and the vanishing line.

### 4.2. Estimation of Intrinsic Parameters

One pair of imaged circular points provides two independent constraints on IAC. Hence three pairs are needed to fully calibrate, which means at three images should be taken. The complete calibration algorithm consists of the following steps:

- Step 1.** Take three images of three separate circles.
- Step 2.** Recover ICs for each image.
- Step 3.** Determine  $\omega$  and obtain  $K$  using the Cholesky factorization.

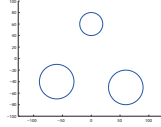


Fig. 6. Three separate circles generated by computer

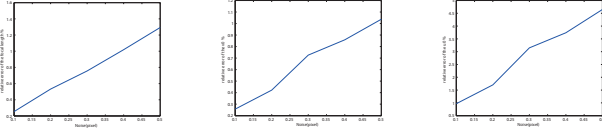


Fig. 7. The relative focal length and image center errors vs. the noise level of the image points.

Table 1. Experimental results with noise 0.3 pixels

Approach	$\alpha f$	$f$	$s$	$u_0$	$v_0$
Ground-truth	1250	900	1.1	320	240
Separate (0.3)	1236.1	893.2	5.5	309.9	241.7
Concentric(0.3)	1249.4	899.8	2.5	319.9	240.3

Table 2. Real experiment results

Approach	$\alpha f$	$f$	$s$	$u_0$	$v_0$
Zhang's	1785.95	1785.95	0	1071.5	711.5
Separate	1729.9	1701.6	-0.7	1094.7	679.1

## 5. EXPERIMENTAL RESULTS

### 5.1. Synthetic Data

In simulations, the simulated camera setup is :  $f=900$ ,  $\alpha f=1250$ , skew  $s=1.1$ , and principal point  $(u_0, v_0)=(320, 240)$ . The image resolution is:  $640 \times 480$ . The model pattern is circles pattern containing three separate circles. In this experiments, we move the camera to obtain three images of the pattern. We choose 100 points on each circle image, and Gaussian noise with zero-mean and  $\sigma$  standard deviation is added to these image points. Ellipses are fitted to these images using a least squares ellipse fitting algorithm [21]. We vary the noise level from 0.1 pixels to 0.5 pixels. For each noise level, we conduct 1000 independent trials, and the final results are shown in average. As we can see from Fig.7, errors increase linearly with the noise level. We also compare our proposed approach with concentric circles [15], we find that there is not too much difference. In Table 1, we show the calibration results with noise 0.3 pixels.



Fig. 8. Images of circles and grid patterns.



Fig. 9. The first image is a vase under a setting of two mirrors, while the second and third images are two views of the reconstructed vase by using our estimated intrinsic parameters.

### 5.2. Real Scene

In the real scene experiment, real images are taken with a Nikon D300s camera. The image resolution is  $2144 \times 1424$ . The images of circles are extracted using Canny edge detector [22], and ellipses are fitted to these images using a least squares ellipse fitting algorithm. The camera is calibrated with the proposed approach. The estimated parameters are listed in Table 2, where the result from the method of Zhang [4] is taken as the ground truth.

To verify the estimated intrinsic parameters, we use the calibrated camera to take a single image of a vase under a setting of two mirrors [23] and reconstruct the vase by using the theory from paper [24]. The first image in Fig. 9 shows the image under a setting of two mirrors. The second and third images in Fig.9 are two views of the reconstructed vase by using our estimated intrinsic parameters. We find that the visual quality of the reconstructed vase is satisfactory.

Note that our proposed method is not suitable for the case that the three circle centers are on the same line. Once the centers are on the same line, the common self-polar triangle from any two of the circles will share one common vertex, which is the vertex at the infinity. Then, the line at infinity can not be recovered.

## 6. CONCLUSION

We have derived a calibration approach based on the the properties of the common self-polar triangles of separate coplanar circles. All steps involved in our approach are linear and easy to implement. We believe that the proposed method in this paper can also be extended to the enclosing but not concentric circles.

## 7. REFERENCES

- [1] Q. Zhou and V. Koltu, "Simultaneous localization and calibration: Self-calibration of consumer depth cameras," in *IEEE Conference on Computer Vision and Pattern Recognition (CVPR)*. IEEE, 2014, pp. 454–460.
- [2] A. Agrawal, "Extrinsic camera calibration without a direct view using spherical mirror," in *IEEE International Conference on Computer Vision (ICCV)*. IEEE, 2013, pp. 2368–2375.
- [3] K.-Y. K. Wong, G. Zhang, and Z. Chen, "A stratified approach for camera calibration using spheres," *Image Processing, IEEE Transactions on*, vol. 20, no. 2, pp. 305–316, 2011.
- [4] Z. Zhang, "A flexible new technique for camera calibration," *Pattern Analysis and Machine Intelligence, IEEE Transactions on*, vol. 22, no. 11, pp. 1330–1334, 2000.
- [5] R. Hartley, "An algorithm for self calibration from several views," in *IEEE Conference on Computer Vision and Pattern Recognition (CVPR)*. IEEE, 1994, vol. 94, pp. 908–912.
- [6] O. D. Faugeras, Q. Luong, and S.J. Maybank, "Camera self-calibration: Theory and experiments," in *Computer Vision–ECCV*. Springer, 1992, pp. 321–334.
- [7] R. Y. Tsai, "A versatile camera calibration technique for high-accuracy 3d machine vision metrology using off-the-shelf tv cameras and lenses," *Robotics and Automation, IEEE Journal of*, vol. 3, no. 4, pp. 323–344, 1987.
- [8] S. J. Maybank and O. D. Faugeras, "A theory of self-calibration of a moving camera," *International Journal of Computer Vision*, vol. 8, no. 2, pp. 123–151, 1992.
- [9] X. Meng, H. Li, and Z. Hu, "A new easy camera calibration technique based on circular points," *Pattern Recognition*, vol. 36, no. 5, pp. 1155–1164, 2003.
- [10] Q. Chen, Y. Wu, and T. Wada, "Camera calibration with two arbitrary coplanar circles," in *Computer Vision–ECCV*, pp. 521–532. Springer, 2004.
- [11] Y. Wu, H. Zhu, Z. Hu, and F. Wu, "Camera calibration from the quasi-affine invariance of two parallel circles," in *Computer Vision–ECCV*, pp. 190–202. Springer, 2004.
- [12] J. S. Kim, P. Gurdjos, and I. S. Kweon, "Geometric and algebraic constraints of projected concentric circles and their applications to camera calibration," *Pattern Analysis and Machine Intelligence, IEEE Transactions on*, vol. 27, no. 4, pp. 637–642, 2005.
- [13] P. Gurdjos, P. Sturm, and Y. Wu, "Euclidean structure from  $n \geq 2$  parallel circles: theory and algorithms," in *Computer Vision–ECCV*, pp. 238–252. Springer, 2006.
- [14] H. Huang, H. Zhang, and Y. M. Cheung, "The common self-polar triangle of concentric circles and its application to camera calibration," in *IEEE Conference on Computer Vision and Pattern Recognition (CVPR)*. IEEE, 2015, vol. 1, pp. 4067–4072.
- [15] H. Huang, H. Zhang, and Y. M. Cheung, "Camera calibration based on the common self-polar triangle of sphere images," in *Computer Vision–ACCV*, pp. 19–29. Springer, 2014.
- [16] R. Hartley and A. Zisserman, *Multiple view geometry in computer vision*, Cambridge university press, 2003.
- [17] J. E. Gentle, *Numerical linear algebra for applications in statistics*, Springer Science & Business Media, 2012.
- [18] F. S. Woods, *Higher geometry*, Applewood Books, 2012.
- [19] L. N. G. Filon, *An introduction to projective geometry*, E. Arnold, 1908.
- [20] J. Semple and G. Kneebone, *Algebraic projective geometry*, Oxford University Press, 1998.
- [21] A. W. Fitzgibbon, M. Pilu, and R. B. Fisher, "Direct least square fitting of ellipses," *Pattern Analysis and Machine Intelligence, IEEE Transactions on*, vol. 21, no. 5, pp. 476–480, 1999.
- [22] J. Canny, "A computational approach to edge detection," *Pattern Analysis and Machine Intelligence, IEEE Transactions on*, vol. 8, no. 6.
- [23] H. Zhang, L. Shao, and K.-Y. K. Wong, "Self-calibration and motion recovery from silhouettes with two mirrors," in *Proc. Asian Conference on Computer Vision*, 2012, vol. 4, pp. 1–12.
- [24] C. Liang and K.-Y. K. Wong, "Robust recovery of shapes with unknown topology from the dual space," *Pattern Analysis and Machine Intelligence, IEEE Transactions on*, vol. 29, no. 12, pp. 2205–2216, 2007.